On the cytoskeleton and soft glassy rheology

Kranthi K. Mandadapu[a,b], Sanjay Govindjee[b,c,*,1], Mohammad R.K. Mofrad[a,*,2]

[a]*Molecular Cell Biomechanics Laboratory, Department of Bioengineering, University of California, Berkeley, CA 94720, USA*
[b]*Department of Civil and Environmental Engineering, University of California, Berkeley, CA 94720, USA*
[c]*Department of Mechanical Engineering and Materials Research Center, ETH Zurich, CH-8092 Zurich, Switzerland*

Abstract

The cytoskeleton is a complex structure within the cellular corpus that is responsible for the main structural properties and motilities of cells. A wide range of models have been utilized to understand cytoskeletal rheology and mechanics (see e.g. [Mofrad, M., Kamm, R., 2006. Cytoskeletal Mechanics: Models and Measurements. Cambridge University Press, Cambridge]). From this large collection of proposed models, the soft glassy rheological model (originally developed for inert soft glassy materials) has gained a certain traction in the literature due to the close resemblance of its predictions to certain mechanical data measured on cell cultures [Fabry, B., Maksym, G., Butler, J., Glogauer, M., Navajas, D., Fredberg, J., 2001. Scaling the microrheology of living cells. Physical Review Letters 87, 14102]. We first review classical linear rheological theory in a concise fashion followed by an examination of the soft glassy rheological theory. With this background we discuss the observed behavior of the cytoskeleton and the inherent limitations of classical rheological models for the cytoskeleton. This then leads into a discussion of the advantages and disadvantages presented to us by the soft glassy rheological model. We close with some comments of caution and recommendations on future avenues of exploration.
© 2008 Elsevier Ltd. All rights reserved.

1. Introduction

The cytoskeleton is an integrated system of biomolecules, providing cellular systems with shape, integrity and internal spatial organization. It is a three-dimensional network consisting of a complex mixture of actin filaments, intermediate filaments and microtubules that are collectively responsible for the main structural properties and motilities of the cell. A wide range of theoretical models have been proposed for cytoskeletal mechanics, ranging from continuum models for cell deformation to actin filament-based models for cell motility (Lim et al., 2006; Mofrad and Kamm, 2006). Numerous experimental techniques have also been developed to quantify cytoskeletal mechanics, typically involving a mechanical perturbation to the cell in the form of either an imposed deformation or force followed by observation of the static and dynamic response of the cell (Fabry et al., 2001; Lim et al., 2006; Mofrad and Kamm, 2006). These experimental measurements along with new theoretical approaches have given rise to several theories for describing the mechanics of living cells. These theories model the cytoskeleton as elastic, viscoelastic, or poro-viscoelastic continua, tensegrity (tension integrity) networks incorporating discrete structural elements that bear compression, porous gels, or most recently as soft glassy materials (SGMs) using the soft glassy rheology (SGR) model (Lim et al., 2006; Mofrad and Kamm, 2006).

Cytoskeletal mechanics plays a key role in many cellular processes and functions, e.g. in cellular mechanotransduction and motility that involves contraction, spreading and crawling. Mechanics also plays an important role in cell division and programmed cell death. In this context, rheological properties of the cytoskeleton are of utmost importance. Several recent studies have reported on the rheological properties of the cytoskeleton, in particular examining the frequency dependency of the storage modulus, $G'(\omega)$, and the loss modulus, $G''(\omega)$. Of particular interest are recent experiments that probe the response of

Corresponding authors.
E-mail addresses: gsanjay@ethz.ch (S. Govindjee),
mofrad@berkeley.edu (M.R.K. Mofrad).
[1]Tel.: +41 44 632 89 46.
[2]Tel.: +1 510 643 8165.

the cytoskeleton in the frequency range of $10^{-2}-10^3$ Hz (Fabry et al., 2001; Bursac et al., 2005; Deng et al., 2006). Inspired by the similarity between experimental data on cells and those reported on SGMs, Fabry et al. (2001) hypothesized that the cytoskeleton is a SGM and can be modeled using the SGR model of Sollich (1998).

SGMs form a class of materials that generically include (liquid) foams, emulsions, slurries and pastes. The dynamics and rheological properties of this class of materials have been reasonably well studied (Mackley et al., 1994; Khan et al., 1988a, b; Mason et al., 1995; Panizza et al., 1996; Hoffman and Rauscher, 1993; Mason et al., 1995) in terms of their linear viscoelastic properties such as storage modulus and loss modulus as a function of frequency. There does not exist a precise definition of a SGM, but it is generally agreed that SGMs possess, at the minimum, the following four properties:

1. They are soft in the sense that they possess mechanical moduli in the Pa to kPa range.
2. Their loss tangent $\tan(\bar{\delta}) = G''(\omega)/G'(\omega)$ is nearly constant for a wide range of frequencies.
3. The frequency dependencies of these moduli are weak power laws of the frequency of the applied load.
4. Under certain conditions they display aging behavior.

The abstract system properties that are claimed to characterize the dynamics of SGMs are the degree of structural disorder and metastability (Sollich et al., 1997). Many experiments have been performed to show evidence of these generic properties, see e.g. Cloitre et al. (2000), Weeks and Weitz (2002) and Ramos and Cipelletti (2001).

One key characteristic of glassy materials is that they are not in thermodynamic equilibrium below their glass transition temperature. Such materials are regarded as solidified supercooled liquids in a metastable non-equilibrium state. Volume-relaxation studies of glassy materials show they undergo slow processes indicating that even below the glass transition temperature, T_g, molecular mobility is not fully suppressed. This gradual evolution affects many properties of the material (Struik, 1966). These properties change with time and the material is said to undergo aging or more precisely *physical aging*. Aging is often measured relative to the time at which the material sample was formed or prepared. Some of the experiments on SGMs in the literature indicate behavior of this type (Cloitre et al., 2000; Ramos and Cipelletti, 2001). Based on such observations of dynamic moduli and aging, Sollich et al. (1997) and Sollich (1998) have developed a theory to model SGMs through a modification of Bouchaud's model of traps and glass phenomenology (Bouchaud, 1992; Monthus and Bouchaud, 1996).

The objective of this paper is to:

1. Provide a concise review of classical linear viscoelasticity.
2. Explore Sollich's SGR model, using the concepts of linear viscoelasticity.

3. Revisit rheological data collected on cultured cells and critically examine its relation to linear viscoelasticity and the SGR model.

In Section 2, we review basic linear rheological representation results which are useful for discussing and understanding the behavior of the cytoskeleton. In Section 3, we review the results of some selected experiments on cytoskeleton. Section 4 examines Bouchaud's model followed by the SGR model proposed by Sollich for modeling SGMs. The comparison of experimental results to the SGR model is made and analyzed in Section 5.

2. Rheological measures: a synopsis

A basic knowledge of rheology is essential for an understanding of the meaning of mechanical experiments performed on cell cultures. In this section we provide a summary of a number of important rheological representation results with added remarks on important modeling assumptions. The aim is to provide a context for a reasoned discussion of the SGR model and a common linguistic platform for discussing and interpreting recent measurements on cell cultures. In the interest of brevity we omit the derivations of the presented formulae and simply refer the interested reader to the classic references of Ferry (1961) and Tschoegel (1989). Not all which we present can be found in these references, but from them, and some modest complex-variable theory, one can derive all the presented results; see also Fuoss and Kirkwood (1941).

2.1. Generic response functional representations

In the interest of illuminating rheological issues, we make our presentation strictly within the geometrically linear theory. In this context, the appropriate strain measure is

$$\boldsymbol{\varepsilon} = \tfrac{1}{2}(\nabla \boldsymbol{u} + \nabla \boldsymbol{u}^{\mathrm{T}}), \tag{1}$$

the symmetric gradient of the displacement field. Within this realm, the simplest material response is stress $\boldsymbol{\sigma} = \hat{\boldsymbol{\sigma}}(\boldsymbol{\varepsilon})$, such that $\int_{t_1}^{t_2} \boldsymbol{\sigma} : \dot{\boldsymbol{\varepsilon}} \, \mathrm{d}t = 0$, when $\boldsymbol{\varepsilon}(t_1) = \boldsymbol{\varepsilon}(t_2)$. The salient feature of this model is that the stress is an instantaneous function of the present value of the strain and is unaffected by the past history. In short, the material is elastic.

In a viscoelastic setting, the stress is dependent on the current and also on the past history of the strain; i.e.,

$$\boldsymbol{\sigma}(t) = \mathop{\mathfrak{S}}_{t' \in (-\infty, t]} (\boldsymbol{\varepsilon}(t')). \tag{2}$$

The stress is said to be a functional of the strain history. Within reasonable continuity assumptions, one can expand the functional as a functional polynomial (Green and Rivlin, 1957). Retaining the leading two terms and assuming the material possesses time translational

invariance (TTI) gives us the classic expression

$$\boldsymbol{\sigma}(t) = \int_{-\infty}^{t} \mathbb{C}(t - t') : \frac{d\boldsymbol{\varepsilon}}{dt'} \, dt'. \tag{3}$$

Here, $\mathbb{C}(t)$ is the fourth order tensorial relaxation kernel. We can additionally split the response into volumetric and deviatoric parts using the standard definitions: $\boldsymbol{\sigma} = p\mathbf{1} + \boldsymbol{s}$, where the deviatoric stress $\boldsymbol{s} = \boldsymbol{\sigma} - \frac{1}{3}\text{tr}(\boldsymbol{\sigma})\mathbf{1}$, the pressure $p = \frac{1}{3}\text{tr}(\boldsymbol{\sigma})$ and $\mathbf{1}$ is the identity tensor. If we make the further assumption of isotropy and elastic bulk response, then, constitutively, we have

$$p = \kappa \text{tr}(\boldsymbol{\varepsilon}),$$

$$\boldsymbol{s}(t) = \int_{-\infty}^{t} G(t - t') \frac{d\boldsymbol{e}}{dt'} \, dt', \tag{4}$$

where κ is the bulk modulus and $\boldsymbol{e} = \boldsymbol{\varepsilon} - \frac{1}{3}\text{tr}(\boldsymbol{\varepsilon})\mathbf{1}$ is the deviatoric strain. Thus, in the linear isotropic setting with elastic bulk response, complete specification of the mechanical rheological properties reduces to the determination of $G(\cdot)$, the so-called (shear) relaxation modulus.

Remarks.

1. It should be emphasized that the representation in Eq. (3) presumes the notion of TTI. This is a very central assumption in most rheological models. Thus care must be taken when trying to interpret results that may pertain to out-of-equilibrium systems where TTI is no longer generally valid. When TTI does not hold, we have the added complication that the relaxation modulus depends not only on relative time $t - t'$ but also explicitly upon absolute time t' — i.e., $G(t - t', t')$.

2. Eqs. (3) and (4) represent models that have a rather broad range of applicability. They are fully independent of any physical model of relaxation and evolution of microstructure. In particular, they are appropriate for stress determination for essentially arbitrary strain histories. This is a point that should be kept in mind when thinking about using rheological models within larger modeling frameworks such as physiological response simulation systems of whole organs or larger systems (Physiome Project, 2007). For these purposes, $G(t)$ is generally required and must be defined over the complete range $t \in [0, \infty)$.

3. The value $G(0)$ is the instantaneous elastic modulus and can be relatively quite high. In fact $G(0) = \infty$ can be mathematically sound but is of course physically unrealistic. For models permitting $G(0) = \infty$, care must be taken in limiting the strength of the singularity so that the required integrals are well defined.

4. $G(t)$ needs to possess the so-called fading memory property (Coleman and Mizel, 1968). To first order, this requires that $G(t) \to G_\infty$, a constant, as $t \to \infty$. If $G_\infty = 0$, then the material is considered a viscoelastic fluid, otherwise a viscoelastic solid.

5. The use of viscoelastic internal variables with differential evolution laws is an alternative to the modeling framework of Eqs. (3) and (4). However, it should be noted that such models are, in principle, a subset of the convolution type models when applied to the geometrically linear case.

2.2. Experimental methods

In theory, the easiest way to determine $G(t)$ is to perform a shear test by imposing a deviatoric step strain $\boldsymbol{e}(t) = \boldsymbol{e}_0 H(t)$, where $\text{tr}(\boldsymbol{e}_0) = 0$ and $H(t)$ is the Heaviside step function. In this case, the measured stress response, $\boldsymbol{s}(t) = G(t)\boldsymbol{e}_0$, directly provides the relaxation function. In practice the imposition of a step strain involves a time constant for inducing the motion and a sampling rate. The net result is that $G(t)$ will only be known in some time interval $[t_{\min}, t_{\max}]$. However, for a complete theory, one must extend the domain to $[0, \infty)$. For a variety of reasons, not the least of which is experimental fidelity, one often employs steady state excitation to determine $G(t)$. In this case, one ends up measuring a close relative of the Laplace transform of $G(t)$. Let $\boldsymbol{e}(t) = \boldsymbol{e}_0 \exp[i\omega t]$, where $i = \sqrt{-1}$ and ω is the frequency of the imposed deformation. Then from Eq. (4), $\boldsymbol{s}(t) = G^*(\omega)\boldsymbol{e}(t)$, where $G^*(\omega)$ is known as the dynamic or complex modulus. $G'(\omega) = \text{Re}(G^*(\omega))$ provides the in-phase stiffness or storage modulus and $G''(\omega) = \text{Im}(G^*(\omega))$ is the out-of-phase stiffness or loss modulus. Their ratio G''/G' is referred to as the loss tangent, $\tan(\bar{\delta}(\omega))$, and is the easiest of all the linear rheological functions to measure as $\bar{\delta}(\omega)$ is just the phase lag of the stress response to the strain excitation. In such experiments $|G^*|$ is the ratio of the peak stress to peak strain. Thus one also has $G' = |G^*| \cos(\bar{\delta})$ and $G'' = |G^*| \sin(\bar{\delta})$.

2.3. Representations

If one desires to change from a steady state representation to a temporal representation or vice versa, then one can employ the well-known interconversion relations that allow one to determine any of the steady state representations from the temporal relaxation function via an integration. Likewise one can also determine the temporal relaxation function via an integration of any of the steady state representations. Both integration procedures, however, are predicated upon an analytic representation of the required integrands over an infinite interval in time or frequency. Having such an analytic representation is often a non-trivial barrier to using such formulae because the integrands are usually determined experimentally over finite intervals. A selection of the most important interconversion relations is presented in part A of the Supplement.

Beyond these two common representations, rheological behavior is often also discussed in terms of spectra. Spectra have the nice advantage that they reveal more clearly the strengths of various relaxation mechanisms in a system.

Completely independent of any assumed physical model, from a purely mathematical perspective, we can express $G(t)$ as

$$G(t) = \int_0^\infty F(\tau)\, e^{-t/\tau}\, d\tau, \qquad (5)$$

where $F(\tau)$ is known as the relaxation-time spectrum for $G(t)$. The magnitude of $F(\cdot)$ at a particular value of τ indicates the importance/strength of relaxation phenomena at that particular time scale. In other words, $F(\cdot)$ is a direct representation of the distribution of relaxation-time scales present in a material. The form is quite general and is not restricted to overall exponential relaxation as one may naively presume from Eq. (5). Note, however, it is common for one to refer to $F(\cdot)$ as a distribution of Maxwell modes. Further, the specification of $F(\cdot)$ allows one to think of relaxation mechanisms in a continuous sense. This is a point which makes good physical sense, if one contemplates the number of possible relaxation mechanisms in any finite size sample. Other common alternatives to Eq. (5) express $G(t)$ in terms of log relaxation-time and relaxation-frequency spectra:

$$G(t) = \int_{-\infty}^\infty H(\log \tau)\, e^{-t/\tau}\, d(\log \tau), \qquad (6)$$

where $H(\log \tau)/\tau = F(\tau)$ and

$$G(t) = \int_0^\infty N(\alpha)\, e^{-t\alpha}\, d\alpha, \qquad (7)$$

where $N(1/\tau)/\tau^2 = F(\tau)$.

Remarks.

1. For simple viscoelastic systems, the spectra are often composed of sums of Dirac distributions but for more complex systems the spectra are continuous functions. As we shall see later, we will be able to gain some insight into the SGR model via a spectral representation.

2. It is possible to interconvert between spectral representations, steady state representations, and temporal relaxation representations. In the part B of the Supplement, we have collected some of the most useful interconversion formulae for such interconversions. Note, however, that the limitation mentioned earlier about interconversion still applies. One always needs an analytic representation of the integrand in the interconversion formula and this is often non-trivial to obtain from experimental methods.

3. Experiments on cytoskeleton

3.1. Equilibrium rheological measurements

Fabry et al. (2001) have performed experiments on the mechanical response of the cellular cytoskeleton with an eye toward soft glassy phenomena and thus we will focus our discussions mainly upon their data. They have obtained the mechanical response of a variety of cells through magnetic twisting cytometry (MTC); see Fig. 1. The details of the experiments are given in Fabry et al. (2001). The dynamic properties G' and G'' of the cytoskeleton's structural response were measured in the experiments; see Fig. 2. It should be remarked that the measured mechanical properties correspond to the linear mechanical behavior of the cytoskeleton embedded inside a cell and are, as such, not the *true* moduli of the cytoskeleton in the sense of a homogenized continuum— though, by linearity, one can reasonably argue that the properties reported should be linearly proportional to the true homogenized continuum moduli of the cytoskeleton.

In the experiments mentioned, the magnetic bead is attached to the cytoskeleton via rigid links between transmembrane integrins and the extracellular molecules (e.g. fibronectins) that are coated on the bead (Fig. 1). A magnetic twisting field introduces a torque causing the bead to rotate and to displace (Fig. 1). The frequency dependence of G' and G'' is then extracted from the structural response at the point of bead attachment. The results are as shown in Fig. 2, where G' increases with
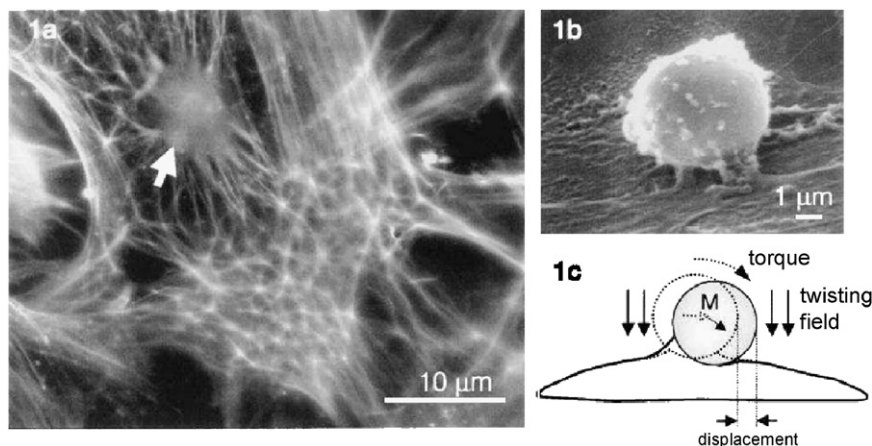

Fig. 1. (a) and (b) Beads attached to the cytoskeleton. (c) The application of magnetic field and the displacement of the bead (reproduced with permission, Fabry et al., 2003).
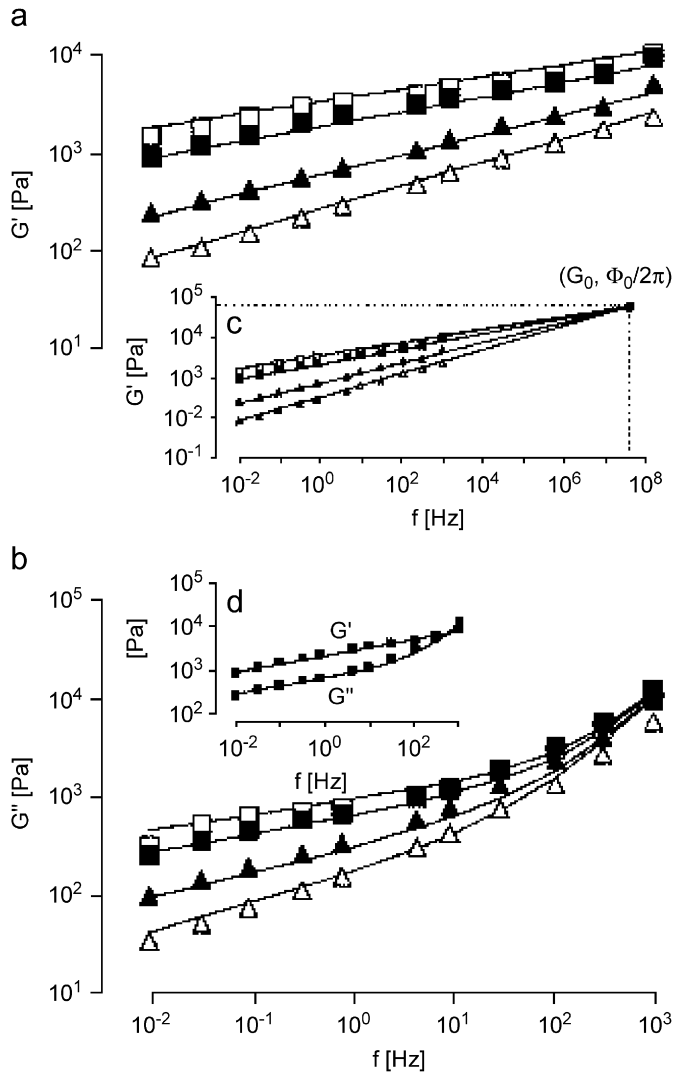
Fig. 2. (a) and (b) G' and G'' as a function of frequency ω for different drug treatments. Under controlled conditions (filled squares), treatment with histamin (unfilled squares), treatment with DBcAMP (filled triangles), treatment with Cytochalasin D (unfilled triangles). The solid lines are fit using Eq. (9) with the values of $\hat{G} = 53.6$ kPa, $\hat{\Phi} = 25 \times 10^7$ rad/s and $\mu = 1.41$ Pa s. (c) Extrapolation of solid lines cross over at $(\hat{G}, \hat{\Phi})$. (d) Dynamic moduli under control conditions (reproduced with permission, Fabry et al., 2003).

increasing frequency, ω, according to a power law $\sim \omega^{x-1}$, with $x = 1.20$ under control conditions. G'' also increases with increasing frequency and follows the same power law in the range of 0.01–10 Hz. Above 10 Hz, however, the same power-law behavior is *not* seen. Similar experiments were performed by manipulating the cells with various drugs in order to create contraction or relaxation in the cytoskeleton and identical qualitative properties were again observed (Fig. 2). G' increased with increasing frequency, ω, as a power law $\sim \omega^{x-1}$ but with different values of x for each treatment. The value of x correlated sensibly to the biochemical activity of the various drugs employed. G'' also increased with increasing frequency with the same power law and same exponent until 10 Hz; above 10 Hz, the behavior changed in a manner similar to what was

observed in the control. It was also noted that the loss tangent in the frequency range 0.01–10 Hz was relatively frequency insensitive and was of the order of 0.1.

Fabry et al. (2003) proposed an empirical relationship for the data they observed from the experiments. They proposed that the stress response $G(t)$ to a unit step strain imposed on the cell at $t = 0$ is

$$G(t) = \mu\delta(t) + \hat{G}\left(\frac{t}{\hat{t}}\right)^{1-x}, \quad t \geqslant 0. \tag{8}$$

Here, $\hat{G}$ is the ratio of stress to the unit strain measured at an arbitrarily chosen time $\hat{t}$, μ is a Newtonian viscosity and $\delta(\cdot)$ is the Dirac delta function. The complex-valued dynamic modulus for this model is

$$
\begin{aligned}
G^*(\omega) = \mathrm{i}\omega\mu + \hat{G}\left(\frac{\omega}{\hat{\Phi}}\right)^{x-1} & \Gamma(2-x) \\
\times \Big[\cos\Big(\frac{\pi}{2}(x-1)\Big) & + \mathrm{i}\sin\Big(\frac{\pi}{2}(x-1)\Big)\Big],
\end{aligned} \tag{9}
$$

where $\hat{\Phi} = \hat{t}^{-1}$.

The four parameters μ, $\hat{G}$, $\hat{\Phi}$ and x can be obtained by statistical analysis of the data and one sees that Eq. (9) is a remarkably good fit of the experimental data; see Fig 2. It is striking that drug interactions only seem to affect x when dealing with a single class of cells. As we shall see in Section 4, the empirically assumed form Eqs. (8) and (9) bear a close resemblance to the SGR model equations.

Remarks.

1. Eq. (9) is mathematically valid for $x < 2$ but the physical restriction (of fading memory) that the relaxation function should not grow with time imposes the limit $x > 1$. Thus, the relation should only be considered valid for $1 < x < 2$ for viscoelasticity.

2. It should also be noted that the relaxation function, Eq. (8), presumes TTI. Thus, the dynamic modulus, Eq. (9) should also be considered to assume TTI; i.e., both relations are only valid near thermodynamic equilibrium.

4. Soft glassy rheology

4.1. Bouchaud's glass model

Bouchaud (1992) originally studied the concepts of structural disorder and metastable configurations in spin-glasses, and later applied his ideas to explain the phenomenology of glassy systems in general (Monthus and Bouchaud, 1996). This model of glass phenomenology is discussed here as it leads directly to Sollich's rheological theory of SGMs. The conformational energy landscape of a finite disordered system is extremely rough, with many local minima corresponding to metastable configurations, or states. These local minima are assumed to be surrounded by high energy barriers. These states can thus be considered as traps which hold the system for certain periods of time τ. The distribution of these trapping times is critical in the quantification of such materials.
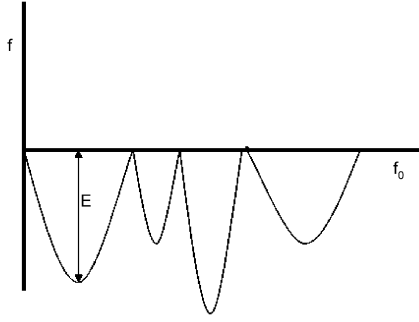
Fig. 3. Energy landscape showing different metastable states after Bouchaud (1992).

A schematic of the energy landscape is given in Fig. 3. Here, f_0 is the energy level below which the states are disconnected. It is the minimum energy required to hop between any two states. It is assumed here that the dynamics between the traps is very fast and the probability to find the system between two metastable states is negligible. The depth of a trap is $E = f_0 - f > 0$. In the model, the abstract space of traps is characterized by a given probability density function $\rho(E)$ for the depth of the traps. Assuming a canonical distribution at temperature $T = \beta^{-1}$, the system can escape from its trap of depth E with a rate $\Gamma_0 e^{-\beta E}$ per unit time, where Γ_0 is an attempt rate. The system chooses a new trap of depth E' with probability $\rho(E')$, with no reference to any spatial structure as may be implied by Fig. 3. Therefore, the probability $P(E, t)$ that one can find the system in a trap of energy depth E at time t evolves in time from an initial condition $P_0(E)$ according to the master balance equation as

$$\frac{\partial P(E, t)}{\partial t} = -\Gamma_0 e^{-\beta E} P(E, t) + \Gamma_0 \Gamma(t)\rho(E), \tag{10}$$

where $\Gamma(t) = \int_0^\infty e^{-\beta E} P(E, t)\, dE$ and a Boltzmann temperature scale is presumed. On the right-hand side of Eq. (10), the first term indicates the rate of probability of hopping out of a trap of energy depth E. The second term indicates the rate of probability of the system falling into a trap of energy depth E. Taken together, these two terms give the rate of change of the probability of finding the system in a trap of depth E.

A normalizable stationary distribution $P_{eq}(E)$ exists at temperature $T = \beta^{-1}$ *if and only if*

$$\Gamma_{eq}(\beta) = \frac{1}{\int_0^\infty e^{\beta E}\rho(E)\, dE} > 0. \tag{11}$$

If we have a normalizable stationary distribution, then $P_{eq}(E)$ is given by

$$P_{eq}(E) = \Gamma_{eq}(\beta)\, e^{\beta E}\rho(E). \tag{12}$$

The condition of normalizability is closely related to the large energy asymptotic behavior of the distribution of traps, which is characterized by the reciprocal (glass transition) temperature:

$$\frac{1}{T_g} = \beta_g = \lim_{E \to \infty} -\frac{\log(\rho(E))}{E}. \tag{13}$$

As pointed out by Bouchaud, three interesting cases arise from this criterion:

1. If $\rho(E)$ decays faster than exponentially at large E, then $T_g = 0$ and a normalizable stationary distribution always exists.
2. If $\rho(E)$ decays slower than exponentially at large E, then $T_g = \infty$ and a normalizable stationary distribution does not exist.
3. If $\rho(E)$ decays exponentially as $e^{-\beta_g E}$ at large E, then T_g is finite and a normalizable stationary distribution exists at temperatures above T_g.

These are the central elements of Bouchaud's abstract model. Before going on to discuss the theory proposed by Sollich, it is important to state that Sollich assumes the existence of a finite non-zero glass transition temperature such that a normalizable stationary distribution exists above a finite T_g and ceases to exist below it.

4.2. SGR theory

Based on Bouchaud's glass model, Sollich et al. (1997) and Sollich (1998) proposed the SGR model. The model pictures a material which consists of a large number of elements that are trapped in *cages* formed by their neighbors. An individual element sees an energy landscape of traps of various depths and, when activated, hops into another trap. Sollich claims that in SGMs, thermal activation is, a priori, very small compared to the typical trap depths. Sollich further claims that activation is due to the interactions between elements; i.e., rearrangements somewhere in the material can cause rearrangements elsewhere. This coupling between elements is unspecified in the model and is solely represented by an effective abstract noise temperature x (Sollich et al., 1997; Sollich, 1998). In reality, it is more likely that the energy barriers are changing due to rearrangements—for example as is known to happen in the yielding of glassy polymers (Argon, 1973). However, since only the ratio of the energy barrier to the temperature appears in the SGR theory, one can argue that one does not have to specify the true state of affairs.

Sollich's evolution equation for the probability of finding an element in a trap of depth E at time t is similar to Eq. (10), except with β replaced by $1/x$. Thus similar to the three cases considered by Bouchaud, to have a normalizable probability distribution, one also has here three cases with x_g being zero, infinite and finite. As mentioned, Sollich assumes that there exists a finite value for the glass transition, denoted here by x_g. For x above x_g, a stationary probability distribution exists and will be reached after a certain amount of time and below x_g the

stationary probability distribution ceases to exist. Thus Sollich assumes the density of traps has an exponential tail, $\rho(E) \sim \exp[-E/x_g]$.

In order to describe material deformation and flow, Sollich further incorporates strain degrees of freedom into Bouchaud's model as a bias on the trapping depths. He restricts himself to a one-dimensional model and introduces a local scalar strain variable l per element. Applying a strain on the material, each element is assumed to deform elastically from the local equilibrium configuration until it reaches a yield point, identified by l_y, from where the element rearranges into a new configuration relaxing the stress in the element. It is assumed that the element fully relaxes taking the strain completely back to zero. As the macroscopic strain γ is increased, l executes a sawtooth-like motion. The yield strain l_y is obtained from the trap depth E, in which the element is located, and thus the yield points have a distribution and not a single value.

Assuming each element to be linearly elastic with an elastic constant k, the stress in the elements evolves as kl, and the elastic energy that can be stored in an element is $\frac{1}{2}kl_y^2$. Assuming that the microscopic strain rate is the same as the macroscopic strain rate, $\dot{\gamma}$, the state of the system at time t is characterized by the probability of finding an element in a trap of energy depth E and a local strain l at time t. The probability evolves as

$$\frac{\partial P(E,l,t)}{\partial t} = -\dot{\gamma}\frac{\partial P}{\partial l} - \Gamma_0\, e^{-(E-\frac{1}{2}kl^2)/x}P + \Gamma_0\Gamma(t)\rho(E)\delta(l),$$

(14)

where

$$\Gamma(t) = \iint e^{-(E-\frac{1}{2}kl^2)/x}P(E,l,t)\,dl\,dE.$$

(15)

On the right-hand side of Eq. (14), the first term represents the change in probability because of the motion in the same energy trap E, while the second and third terms have the same meaning as described earlier. Note that the third term now contains a $\delta(l)$ function, due to the assumption that the local strain becomes zero immediately after the relaxation. It must be remarked that the energy well chosen is uncorrelated with its previous one. The average non-dimensionalized (by Γ_0) yielding rate is given by Eq. (15).

Finally, the rheological response, which is the macroscopic stress, is obtained as the expectation value of the local stresses:

$$\sigma = \iint kl P(E,l,t)\,dl\,dE.$$

(16)

As Sollich importantly points out, the *effective noise temperature* x is not a parameter that we can easily tune from outside; rather, it is to be determined self-consistently by the interactions in the system.

4.3. SGR linear relaxation function

As detailed in part C of the Supplement one can solve Eq. (16) to obtain a nonlinear viscoelasticity model—i.e., a model where the rate of viscous relaxation depends upon the degree of perturbation from equilibrium as measured by strain. This model can be further linearized to yield a small strain linear viscoelastic model. Central to this procedure is the assumption that the material is near equilibrium and that one can use the equilibrium probability distribution as an initial condition. The end result yields expressions for the above x_g, small strain, near equilibrium relaxation function and complex modulus as

$$G(t) = k\Gamma_0\left(\frac{x}{x_g} - 1\right)\int_{1/\Gamma_0}^{\infty} e^{-t/\tau}(\Gamma_0\tau)^{-x/x_g}\,d\tau,$$

(17)

where $\tau = (1/\Gamma_0)\exp(E/x)$ and represents the average trapping time in a particular well in the SGR model. The dependency of the dynamic modulus on frequency is

$$G^*(\omega) = G'(\omega) + iG''(\omega) = i\omega$$
$$\times \int_0^{\infty} e^{-i\omega t}kG_0(\Gamma_0 t)\,dt = k\Gamma_0\left(\frac{x}{x_g} - 1\right)$$
$$\times \int_{\frac{1}{\Gamma_0}}^{\infty}\frac{i\omega\tau}{1+i\omega\tau}(\Gamma_0\tau)^{-x/x_g}\,d\tau.$$

(18)

Remarks.

1. In reference to part B of the Supplement, Eqs. (17) and (18) show that the linearized near equilibrium SGR model is mathematically equivalent to a system (of Maxwell elements) with a continuous power-law distribution of relaxation times, $F \sim \tau^{-x/x_g}$, with a lower relaxation-time cut-off of $1/\Gamma_0$. In relaxation space, we see that this model has a linear distribution on a $\log - \log$ scale; i.e., $\log(H) \sim \log(\tau)$. Such a behavior is often associated with self-similar phenomena.
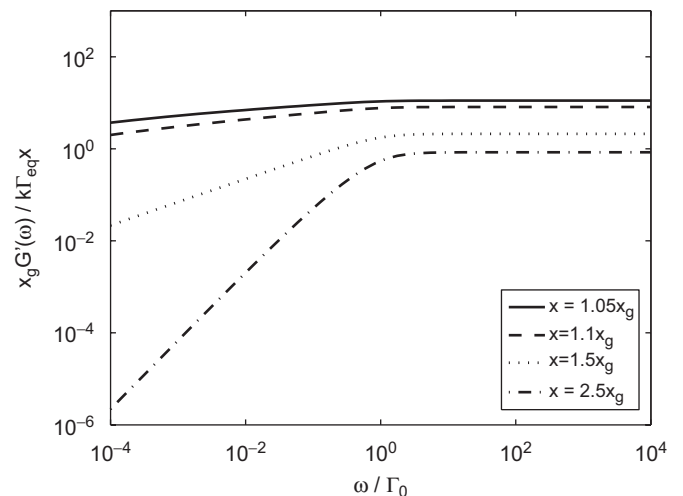

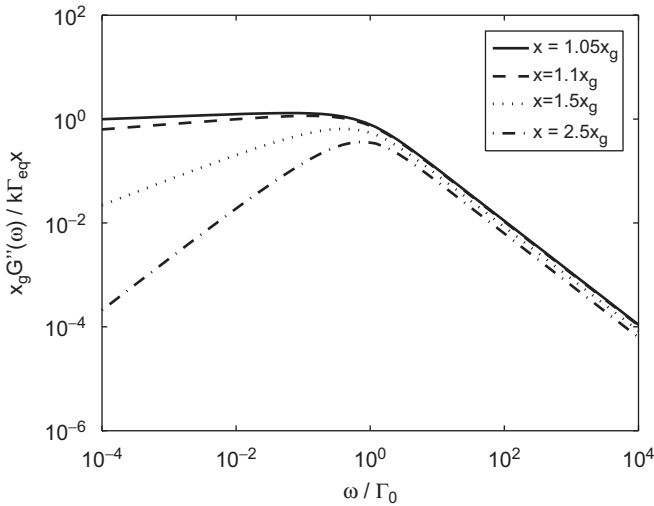Fig. 4. G' variation with frequency ω for $\frac{x}{x_g} = 1.05$, 1.1, 1.5, 2.5.

Fig. 5. G'' variation with frequency ω for $\frac{x}{x_g} = 1.05, 1.1, 1.5, 2.5$.

2. The behavior of the dynamic modulus is most easily seen via simple numerical simulation; see Figs. 4 and 5. One observes for frequencies of order 1 and less relative to the attempt frequency, Γ_0, that:

$$G'(\omega) \sim \begin{cases} \left(\dfrac{\omega}{\Gamma_0}\right)^2 & \text{for } 3 < \dfrac{x}{x_g} \text{ and } 10^{-4} < \dfrac{\omega}{\Gamma_0} < 1 \\[2ex] \left(\dfrac{\omega}{\Gamma_0}\right)^{(x/x_g)-1} & \text{for } 1 < \dfrac{x}{x_g} < 3 \text{ and} \\[2ex] & 10^{-4} < \dfrac{\omega}{\Gamma_0} < 1, \end{cases}$$

(19)

$$G''(\omega) \sim \begin{cases} \left(\dfrac{\omega}{\Gamma_0}\right) & \text{for } 2 < \dfrac{x}{x_g} \text{ and } 10^{-4} < \dfrac{\omega}{\Gamma_0} < 1, \\[2ex] \left(\dfrac{\omega}{\Gamma_0}\right)^{(x/x_g)-1} & \text{for } 1 < \dfrac{x}{x_g} < 2 \text{ and} \\[2ex] & 10^{-4} < \dfrac{\omega}{\Gamma_0} < 1. \end{cases}$$

(20)

The interesting regime is the range where x/x_g lies between 1 and 2. In this range, G' and G'' have a constant ratio and both vary as $\omega^{(x/x_g)-1}$.

3. The theoretical predictions are also plotted for frequencies above the attempt frequency to illustrate the models behavior over a wide range. However, one should note that physically the model likely makes little sense at such frequencies. A central element of the SGR model is that the local behavior is elastic. This requires a separation of time scales between the loading frequency and the attempt rate frequency. If the loading frequency is of the order of the attempt frequency then the local behavior cannot sensibly be modeled with an elastic model. In this case, a local viscoelastic response would be more appropriate, which then greatly complicates the evaluation of the

theory. As a rule of thumb, the SGR model should be limited to applications where $\omega < \Gamma_0/10$; this will guarantee the needed separation of time scales.

5. Comparison of cytoskeleton and soft glassy rheology

In Fabry et al. (2001) it has been observed that the cytoskeleton possess the properties of a SGM and thus there is the possibility of modeling the cytoskeleton using the SGR model of Sollich and to learn more about its functioning. Here we examine where this modeling assumption succeeds and where further efforts are needed.
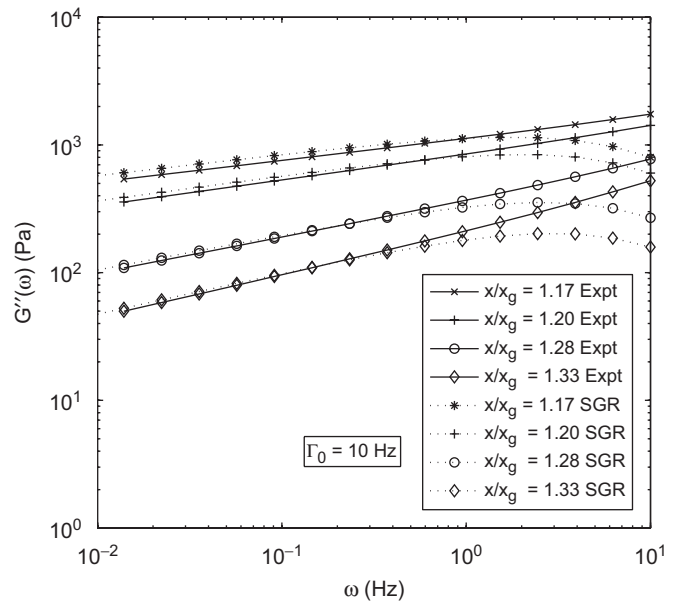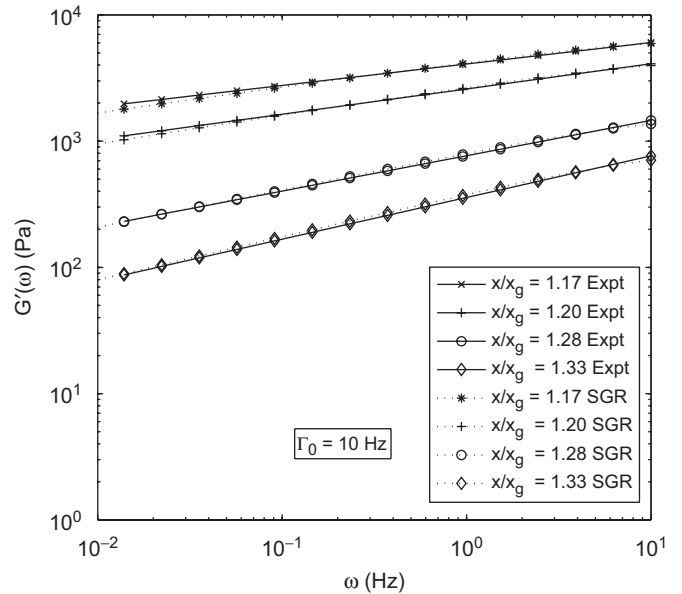

Fig. 6. Regression fit of the SGR model to the data of Fabry et al. (2003). Solid lines represent the experimental data and the remaining curves represent the model fit. In all cases, $\Gamma_0 = 10$ Hz. The fitted local elasticities are given as 6.7, 4.4, 1.5, 0.78 kPa for the cases of x/x_g of 1.17, 1.20, 1.28, 1.33, respectively.

5.1. Viscoelastic function comparison

The data in Fabry et al. (2001, 2003) was originally fit quite well using the empirical model in Eq. (9) and produced a result that showed that drug interactions only changed the effective noise parameter and not the other model parameters. This astonishing selectivity is very attractive in terms of model building. For direct comparison to the SGR model we can fit Eq. (18) to the same data. In this fitting process we can use the slope of the data to determine x/x_g and then we can use regression to determine k and Γ_0 in the SGR model. Our best fit is found using a single $\Gamma_0 \approx 10\,\mathrm{Hz}$; see Fig. 6. Unfortunately, the drug treatments affect more than one parameter in the SGR model unlike what was seen with the empirical model. In the SGR model we find that the local elasticities also vary with drug treatment. The variation of the local elasticities with drug treatment; however, is still quite sensible relative to the biochemical activities of the drugs used.

5.1.1. Storage modulus

The storage modulus G' from the data and the SGR model match each other well even up to $\omega/\Gamma_0 \sim 1$ where we cannot expect good agreement. This promising behavior also gives us the interpretation that mechanistically the cytoskeleton possesses a linear log–log relaxation-time spectrum and further that for the storage modulus the cytoskeleton is well modeled by the SGR model with an initial equilibrium noise state above the glass transition. It is further possible to have good agreement for the storage modulus over the entire range of the data up to 1000 Hz by changing Γ_0 to 1000 Hz. However, this causes problems with the fitting of the loss modulus; see Fig. 7.

5.1.2. Loss modulus

A comparison of the G'' behavior of the SGR model and the data yield good results with the choice of $\Gamma_0 = 10\,\mathrm{Hz}$. We can see that the SGR prediction is quite close to the data and that the two do not deviate until one reaches frequencies $\omega/\Gamma_0 \geqslant \frac{1}{10}$ and in this range we have no right to expect that the SGR model will produce reasonable results. It should be observed that the more glassy the system is, the better the match is to the SGR model. The higher noise systems seem to start to deviate from the SGR model at lower values of ω/Γ_0. One could consider adjusting Γ_0 to a lower value for these systems but then the very good fit for the storage modulus will be limited by this low value of the attempt frequency; see Fig. 4. It would be an interesting exercise to try and find an independent means of assessing the local attempt frequency. This would then allow for a more reasoned discussion of the fit of the storage and loss modulus to the SGR model.

Remarks.

1. The above comparisons with the SGR model all assume that the systems are near equilibrium. They are based on
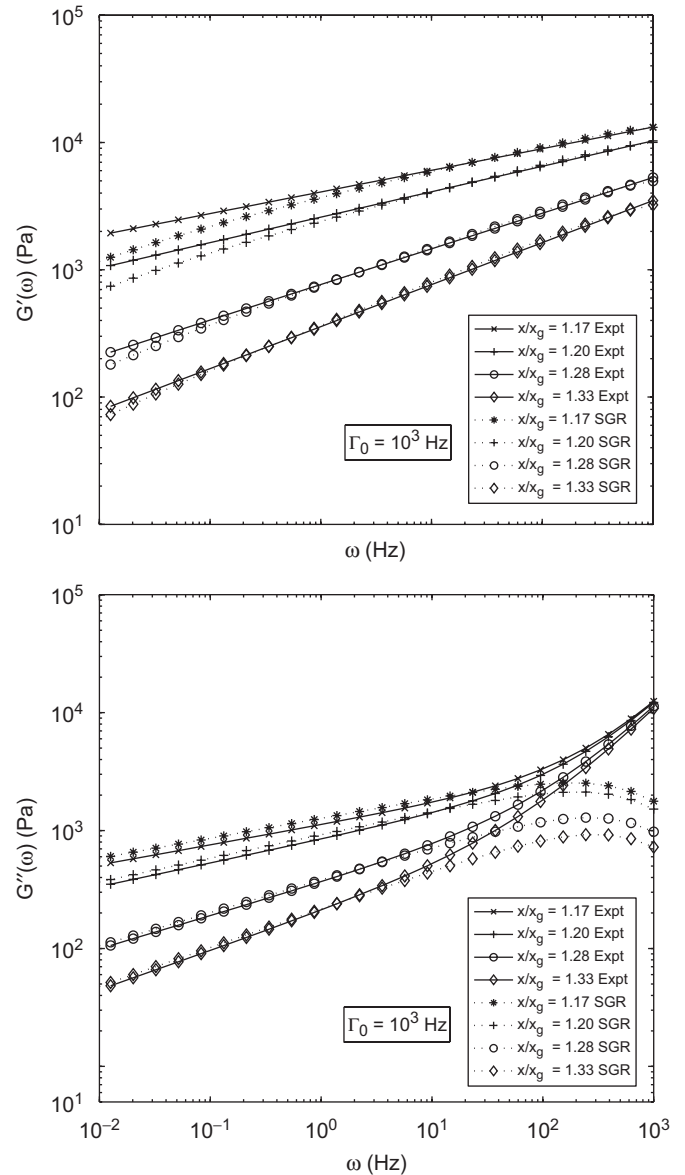

Fig. 7. Regression fit of the SGR model to the data of Fabry et al. (2003). Solid lines represent the experimental data and the remaining curves represent the model fit. In all cases, $\Gamma_0 = 1000\,\mathrm{Hz}$. The fitted local elasticities are given as 14.9, 11.1, 5.5, 3.6 kPa for the cases of x/x_g of 1.17, 1.20, 1.28, 1.33, respectively.

the presumption that the strains are small and that the initial probability distribution of states is the equilibrium distribution. If the system is not near equilibrium at the time of the measurements then it can be quite difficult to interrogate the SGR model for its predictions. If the deviations from equilibrium are due to large strains away from an equilibrium state then there are some possibilities for solving the SGR equations. Efforts in this direction can be found in Trepat et al. (2007) where good agreement between the SGR model and cytoskeleton data are seen.

2. The data discussed was originally fit in Fabry et al. (2001, 2003) using the empirical relation Eq. (9). A comparison of this empirical relation with the SGR model equations shows that they have effectively utilized a Γ_0 on

the order of 10^8 Hz. This provides for a good fit to the storage modulus data over its entire range but then suggests that the loss modulus data begins to deviate from the SGR model around $\omega/\Gamma_0 \approx 10^{-7}$—well within the expected range of validity of the SGR model. Thus the slower rate of 10 Hz proposed above seems to provide a more consistent correspondence between the SGR model and the data— even if the range of matching is somewhat reduced.

5.2. Non-equilibrium issues: aging

In the previous section, the behavior discussed, storage and loss moduli for the cellular systems in Fabry et al. (2003), can be explained in three nearly equivalent ways: (1) using the empirical fitting equation Eq. (9), (2) using the SGR model, or (3) by a classical rheological model with a linear log–log relaxation-time spectrum. The three options have their pluses and minuses but one can say that option (2) provides the most flexibility in that it also allows for nonlinear viscoelastic behavior and further presents the possibility of realistically modeling behaviors associated with noise temperatures below x_g. This added feature of the SGR model is attractive as recent measurements have begun to show such behaviors in the cytoskeleton. Generically, these features go by the names of *aging* and *rejuvenation*. It should be emphasized that there are two basic types of aging/rejuvenation behavior present in the SGR model:

1. One type of aging/rejuvenation behavior is due to large strain effects in the effective material clock; see e.g. Bursac et al. (2005), Trepat et al. (2007), Reese and Govindjee (1998) and Govindjee and Reese (1997). These effects manifest themselves in the SGR model via the nonlinear material clock; see Eq. (C.6) in part C of the Supplement. In this situation, straining pushes the material state far from equilibrium and nonlinear relaxation takes place to bring the material back to equilibrium (the rejuvenation). If the time scales are sufficiently separated, then aging type behavior will be observed; i.e., one will see time dependent behavior in storage and loss modulus measurements over the time period required to bring the system back near equilibrium. Such aging/rejuvenation behaviors can be present at noise temperatures above x_g and it has been shown in Trepat et al. (2007) to be consistent with the SGR model.
2. The second type of aging behavior occurs strictly below x_g. Below x_g a normalizable stationary probability distribution does not exist in the SGR model. Thus the state of the system constantly evolves and the properties of the system constantly change or age. This is the usual type of aging that is referenced in literature dealing with glassy systems. It deals strictly with the evolution of the sub-scale dynamics of the material which do not possess a steady state solution.

As mentioned, for $x < x_g$, the SGR model displays aging characteristics, and, in recent experimental results by

Bursac et al. (2005), indicators of glassy aging in the cytoskeletal mechanical response have been measured in cultured cells. One of the basic experiments performed showed that a tracer bead attached to the cytoskeleton diffuses in a manner that is inconsistent with equilibrium diffusive behavior (Stokes–Einstein behavior); see Figs. 3 and 4 in Bursac et al. (2005). This behavior occurs in unperturbed cells that one would nominally think of as being in equilibrium. The implication of the observed time scaling behavior is that the cell culture is actually below its glass transition temperature. This conclusion is, however, inconsistent with the fact that one can well fit storage and loss modulus data for the cytoskeleton using a noise temperature $x > x_g$. One possible explanation for this inconsistency is that the cell cultures in Bursac et al. (2005) were above x_g but prepared out-of-equilibrium. The required degree of out-of-equilibrium preparation can be estimated using the creep experiments in Bursac et al. (2005); see their Fig. 1. This data show that the system displays out-of-equilibrium behavior for over 8000 s. This implies that the system has a high degree of energy well occupancy for states with $E/x > \ln(8000\Gamma_0) \approx 11.2$, where we have assumed that $\Gamma_0 = 10$ Hz. In equilibrium, only about 10% of the system should occupy states with $E/x > 11.2$, assuming $x/x_g = 1.2$. The likelihood of this occurring is finite but low since it would require moving the system out of 90% of the states which it preferentially occupies in equilibrium. Thus we are left with an inconsistency between the data and the SGR model. In order to settle this question, one would need experiments designed to measure the underlying dynamic structure of the SGR model.

6. Concluding remarks

The modeling of the rheological behavior of the cytoskeleton is a challenging subject that has recently been the subject of a number of studies. In this article we have endeavored to provide the reader with a concise review of the structure of classical linear rheological modeling, the SGR model, and the relation of these two frameworks to some recent rheological measurements on the mechanical response of the cytoskeleton of cultured cells.

The measured data are of several types: (1) frequency sweep measurements of storage and loss moduli at low amplitude motion, (2) measurement of the local Brownian dynamics of the cytoskeleton and (3) probes of the relaxation behavior of the cytoskeleton after large perturbations. If we wish to be able to treat all three types of data in a single model then we require a model that incorporates not only linear and nonlinear viscoelastic behavior but one that also contains a sub-scale dynamic component. This sub-scale dynamic component is required if we are to be able to model Brownian motion type experiments. In this regard the most promising modeling framework available to us is the SGR model of Sollich.

As shown above, the SGR model can be interpreted above the glass transition noise temperature as a classical linear rheological system with a linear log–log relaxation-time spectrum with a slow mode cut-off time when the initial sub-scale energy distribution is taken as the equilibrium one. This feature allows the SGR model to model data of type (1). Also this model has the added feature of being able to predict data of type (3) due to its embedded nonlinear clock. Analysis of the model in this range of motion is somewhat complicated due to the structure of the equations but qualitatively it has been shown to correlate well with experimental data. The SGR model has the further added feature that it is capable to predicting sub-scale dynamics, type (2) data, and in particular for noise temperatures below the glass transition. These predictions are rather dependent upon assumptions about the initial probability distribution for the system but within reasonable assumptions the model provides testable predictions. It is here, however, that we find some difficulties in employing the SGR model as a model for the cytoskeleton's mechanical response. The bead tracer data indicates that the cytoskeleton is in a glassy condition due to violations of the Stokes–Einstein rule. But one has, on the other hand, the fact that types (1) and (3) data are well explained by the SGR model using noise temperatures above equilibrium. The contradiction is difficult to resolve even if one is willing to accept the possibility of a non-equilibrium system preparation above the glass transition noise temperature.

Due to the strong positive predictions of the SGR model, it is worthwhile to consider appropriate means to reconcile the contradictory observations of simultaneous above and below glass transition behavior. In our opinion, further efforts should be devoted to independently measuring the sub-elements of the SGR model—in particular the attempt rate and the evolution of the internal probability distribution. In performing such measurements, care should be taken to probe within the linear and nonlinear relaxation regimes as determined by the effective clock of the material. As a closing word of caution, we should, however, mention that none of these modeling efforts account explicitly for the fact that the cytoskeleton exists within a living cell with its own internal energy source. It is quite conceivable that this energy source serves to constantly perturb the system's probability distribution away from the assumed stationary one.

Conflict of interest statement

This statement is to declare that we, Kranthi K. Mandadapu, Sanjay Govindjee, and Mohammad R.K. Mofrad, the authors of manuscript *On the cytoskeleton and soft glassy rheology* do not possess any financial relationships that might bias our work. We hereby declare that no conflict of interest exists in our work.

Appendix A. Supplementary data

Supplementary data associated with this article can be found in the online version at doi:10.1016/j.jbiomech.2008.02.014.

References

Argon, A., 1973. Theory for low-temperature plastic-deformation of glassy polymers. Philosophical Magazine 28, 839–865.

Bouchaud, J., 1992. Weak ergodicity breaking and aging in disordered systems. Journal de Physique I France 2, 1705–1713.

Bursac, P., Lenormand, G., Fabry, B., Oliver, M., Weitz, D., Viasnoff, V., Butler, J., Fredberg, J., 2005. Cytoskeletal remodeling and slow dynamics in the living cell. Nature Materials 4, 557–561.

Cloitre, M., Borrega, R., Leibler, L., 2000. Rheological aging and rejuvenation in microgel pastes. Physical Review Letters 85, 4819–4822.

Coleman, B., Mizel, V., 1968. On general theory of fading memory. Archive for Rational Mechanics and Analysis 29, 18–31.

Deng, L., Trepat, X., Butler, J., Millet, E., Morgan, K., Weitz, D., Fredberg, J., 2006. Fast and slow dynamics of the cytoskeleton. Nature Materials 5, 636–640.

Fabry, B., Maksym, G., Butler, J., Glogauer, M., Navajas, D., Fredberg, J., 2001. Scaling the microrheology of living cells. Physical Review Letters 87, 14102.

Fabry, B., Maksym, G., Butler, J., Glogauer, M., Navajas, D., Taback, N., Millet, E., Fredberg, J., 2003. Time scale and other invariants of integrative mechanical behavior in living cells. Physical Review E 68, 041914.

Ferry, J., 1961. Viscoelastic Properties of Polymers. Wiley, New York.

Fuoss, R., Kirkwood, J., 1941. Electrical properties of solids. VIII. Dipole moments in polyvinyl chloride–diphenyl systems. Journal of the American Chemical Society 63, 385–394.

Govindjee, S., Reese, S., 1997. A presentation and comparison of two large deformation viscoelasticity models. ASME Journal of Engineering Materials and Technology 119, 251–255.

Green, A., Rivlin, R., 1957. The mechanics of non-linear materials with memory. Part I. Archive for Rational Mechanics and Analysis 1, 1–21.

Hoffman, H., Rauscher, A., 1993. Aggregating systems with a yield stress value. Colloid Polymer Science 271, 390–395.

Khan, S., Prudhomme, R., Graessley, W., 1988a. Rheology of concentrated microgel solutions. Rheologica Acta 27, 531–539.

Khan, S., Schnepper, C., Armstrong, R., 1988b. Foam rheology: III. Measurement of shear flow properties. Journal of Rheology 32, 69–92.

Lim, C., Zhou, E., Quek, S., 2006. Mechanical models for living cells. Journal of Biomechanics 39, 195–216.

Mackley, M., Marshall, R., Smeulders, J., Zhao, F., 1994. The rheological characterization of polymeric and colloidal fluids. Chemical Engineering Science 49, 2551–2565.

Mason, T., Bibette, J., Weitz, D., 1995. Elasticity of compressed emulsions. Physical Review Letters 75, 2051–2054.

Mason, T., Weitz, D., 1995. Linear viscoelasticity of the colloidal hard sphere suspensions near the glass transition. Physical Review Letters 75, 2770–2773.

Mofrad, M., Kamm, R., 2006. Cytoskeletal Mechanics: Models and Measurements. Cambridge University Press, Cambridge.

Monthus, C., Bouchaud, J., 1996. Models of traps and glass phenomenology. Journal of Physics A 29, 3847–3869.

Panizza, P., Roux, D., Vuillaume, V., Lu, C., Cates, M., 1996. Viscoelasticity of onion phase. Langmuir 12, 248–252.

Physiome Project, 2007. ⟨http://www.physiome.org⟩.

Ramos, L., Cipelletti, L., 2001. Ultraslow dynamics and stress relaxation in the aging of a soft glassy system. Physical Review Letters 87, 245503.

Reese, S., Govindjee, S., 1998. A theory of finite viscoelasticity and numerical aspects. International Journal of Solids and Structures 35, 3455–3482.

Sollich, P., 1998. Rheological constitutive equation for a model of soft glassy materials. Physical Review E 58, 738–759.

Sollich, P., Lequeux, F., Hebraud, P., Cates, M., 1997. Rheology of soft glassy materials. Physical Review Letters 78, 2020–2023.

Struik, L., 1966. Volume relaxation in polymers. Rheologica Acta 5, 303–310.

Trepat, X., Deng, L., An, S., Navajas, D., Tschumperlin, D., Gerthoffer, W., Butler, J., Fredberg, J., 2007. Universal physical responses to stretch in the living cell. Nature 447, 592–596.

Tschoegel, N., 1989. The Phenomenological Theory of Linear Viscoelastic Behavior: An Introduction. Springer, Berlin.

Weeks, E., Weitz, D., 2002. Subdiffusion and the caging effect near the colloidal glass transition. Chemical Physics 284, 361–367.